Carcinogenesis Advance Access published September 8, 2005

CB
Received June 9, 2005; revised August 26, 2005; accepted September 3, 2005

The Time and Spatial Effects of Bystander Response in Mammalian Cells Induced by Low Dose Radiation

Burong Hu[1], Lijun Wu[1*], Wei Han[1], Leilei Zhang[1], shaopeng Chen[1], An Xu[1], Tom K Hei[2] and Zengliang Yu[1*]

[1] *Key Laboratory of Ion Beam Bioengineering, Institute of Plasma Physics, Chinese Academy of Sciences, Hefei 230031, People's Republic of China,*

and

[2] *Center for Radiological Research, College of Physicians and Surgeons,Columbia University, New York 10032, USA*

[*] Corresponding Authors

Number of figures submitted：5

Suggested running header: The time and spatial effects of bystander response

Corresponding Authors: Lijun Wu & Zengliang Yu
Address: P. O. Box 1126, Hefei, Anhui 230031, P. R. China
Phone Number: 86-551-5591602
Fax Number: 86-551-5591310
Email Address: ljw@ipp.ac.cn

Abbreviations: DSBs, DNA double-strand breaks; γ-H2AX, phosphorylated form of H2AX; ROS, reactive oxygen species; GJIC, gap junctional intercellular communication; RIBE, radiation-induced bystander effects; SCE, sister chromatid exchanges; MN, micronucleus.

ABSTRACT

Bystander effects induced by low dose of ionizing radiation have been shown to be widely existed in many cell types and may have a significant impact on radiation risk assessment. Though many studies have been reported on this phenomenological observation, the mechanisms underlying this process are not clear, especially on the questions of how soon after irradiation the bystander effects can be initiated and how far this bystander signal can be propagated once it started. DNA double-strand breaks (DSBs) induced by ionizing radiation or carcinogenic chemicals can be visualized *in situ* using γ-H2AX immunofluorescent staining. Our previous studies have shown that *in situ* visualization of DSBs could be used to assess irradiation-induced extranuclear/extracellular (bystander) effect at an early stage after irradiation. In the present studies, we used this method to investigate the time and spatial effects of damage signals to un-irradiated bystander cells. The results showed that increased DSBs in irradiated and unirradiated bystander areas could be visualized 2min after radiation and reached its maximum 30min after radiation. The average levels of DSBs formation at 30 minutes post 1cGy irradiation in the irradiated and unirradiated bystander areas were 3 and 2 folds higher than those of the sham-irradiated control cells, respectively. Afterwards, the formation of DSBs declined with incubation time and maintained steady for at least 6 hrs at a level which was statistically higher than their controls. The results also showed that the bystander signal derived from irradiated cells could be transferred to anywhere in the dish and the percentage of DSBs in the cells in unirradiated bystander cells was not dependent on the dose delivered. Moreover, the fraction of DSBs positive cells in unirradiated bystander areas showed a time dependent increases based on its distance to irradiated area at very early stage post irradiation. Both lindane and DMSO significantly suppressed the yield of DSBs in the cells of unirradiated bystander areas, which suggest that gap junctional intercellular communication (GJIC) and reactive oxygen species (ROS) played important roles in the induction of the bystander effects both in irradiated and unirradiated bystander areas.

INTRODUCTION

The phenomenon known as "radiation-induced bystander effects" (RIBE) was described almost six decades ago since the earlier work of Kotval & Gray, which showed that α-particles which passed close, but not through the chromatid thread had a significant probability of producing chromatid breaks or chromatid exchanges in cells (1). The modern day definition of RIBE, however, derived mainly from the work based on micro-dosimetric principles conducted more than a decade ago by Nagasawa and Little (2), which indicated that an enhanced frequency of sister chromatid exchanges (SCE) was observed in 20-40% of Chinese hamster ovary cells when the culture was exposed to a low dose of α-particles such that only 0.1-1% of the cells' nuclei were expected to be traversed by a particle track. Since then, considerable evidence has accumulated for the existence of these RIBE in which cells that have not directly been hit by irradiation demonstrate many of the same effects as irradiated cells, using endpoints such as cell killing, micronucleus (MN) induction, mutation, oncogenic transformation, and changes in cellular growth pattern (1, 3, 4). RIBE has been observed in a number of different cell types irrespective of the type of radiation exposure. Both high LET α-particles (5-9) and low LET γ-irradiation (10-12) have been shown to induce RIBE.

While bystander effects have been well demonstrated with a variety of biological endpoints in both human and rodent cell lines, as well as in three-dimensional tissue samples (13), the kinetics and mechanisms of the phenomenon are not clear, especially the time and spatial effects on how the bystander signal is transferred. Belyakov *et al*. reported that there was a 2-3 fold increase in micronucleus level in an unexposed quadrant of the dish 3 days after 200 cells within one quadrant (5×5 mm^2) of the dish were exposed to α-particles (14). Here 3 days was chosen as the scoring time that represented the peak formation of micronucleatedncells in the population in their studies. Using the ultrasoft X-ray microprobe available at the Gray Cancer Institute where only a single V79 cell within the population was targeted, Schettino *et al*. observed that the cell killing occurred among the unirradiated area within a distance of ～3mm radius from the one targeted cell 3 days after the dishes were revisited (15). Recently, using the bound proliferating cell nuclear antigen (PCNA) in nuclei of cells as an *in situ* bystander endpoint, Hill *et al*. observed an increase in expression of PCNA among unirradiated cells in the shielded area of the

dish 4h after irradiation with a 0.4cGy dose of α-particles (16). There is evidence that bystander cells accumulate phosphorylated (activated) forms of ERK1/2, JNK, p38, and the upstream Raf-1 kinase within 1 min after the cultures exposed to a mean dose of 5cGy α particles (7). Consistent with the occurrence of DNA damage in the irradiated cultures, detectable accumulation of p53 was noted by 15 min after irradiation and an increase in phosphorylation of Ser15 on p53 was also observed by 1 min postirradiation. Though these studies suggested some sort of the time and distance effects of bystander response, the results were estimated based on dosimetric calculation. It is not known, for example, how soon after irradiation the bystander effects can be initiated in the unirradiated bystander area. It is certainly, not known how far this signal can be propagated once it started since the endpoints used in previous studies mostly reflect the phenomenon appearing several hours or several days post-radiation.

DNA double-strand breaks (DSBs) are considered to be the most relevant lesion for the deleterious effects of ionizing radiation (17, 18). One of the earliest steps in the cellular response to DSBs is the phosphorylation of serine 139 of H2AX, a subclass of eukaryotic histone proteins that are part of the nucleoprotein structure called chromatin (19). Using a fluorescent antibody specific for the phosphorylated form of H2AX (γ-H2AX), discrete nuclear foci can be visualized at sites of DSBs *in situ*, either induced by exogenous agents such as ionizing radiation (20,21) or generated endogenously during programmed DNA rearrangements (22-24). Several studies have shown consistently that a γ-H2AX focus represents a DSB and that γ-H2AX foci formation can be used to measure the repair of individual DSBs in human cells (22, 24). The induced DSBs are visible as early as 1min after irradiation (20). The formation of DSBs becomes distinct and reaches maximum 10-30min after irradiation, and then decreases to ～30% of this level 1h later (20). Thus, this *in situ* assay, based on immunochemistry of γ-H2AX, can reflect the early events of damage induced by IR and may provide time dependent information of bystander effects. Our previous studies demonstrated that *in situ* visualization of DSBs can be used to assess early-stage event of irradiation-induced extranuclear/extracellular (bystander) effects (25).

In the present studies, to analyze the time and spatial effects of the bystander signal transfer and its kinetics at an early stage postirradiation，we exposed only partial or ～25% of cells plated onto rectangular dishes (10×6 mm^2, Figure 1) to α-particles. The distances that bystander signal traveled, together with the degree of bystander effect on unirradiated cells, were investigated using the DSBs assay. The use of rectangular dishes provides an opportunity to divide the

non-irradiated area into equal, progressive quadrants from the irradiated area (2.5×6 mm^2).

MATERIALS AND METHODS

Cell Culture and Alpha-particles Irradiation

AG1522 normal human diploid skin fibroblasts, received as a kind gift from Dr. Barry Michael (Gray Laboratory, UK), were maintained in α-Eagle's minimum essential medium (Gibco) supplemented with 2.0mM L-glutamine and 20% FBS (Hyclone) plus 100μg/ml streptomycin and 100U/ml penicillin (Gibco) at 37□ in a humidified 5% CO_2 incubator. For irradiation, approximately 1×10^4 exponentially growing AG1522 cells in passage 11-14 were seeded into each specially designed rectangular dish (internal area: $10\times6mm^2$) consisting of a 3.5μm thick mylar film bottom on which cells attached. The culture medium was replaced every 2 days until the cells developed into a confluent monolayer before irradiation. At that time, about 92% of the cells were in G0-G1 as determined by flow cytometry. The cells were synchronized in G0-G1 by confluent, density inhibition of growth to eliminate complications in the interpretation of the results (7). The average energy of α-particles derived from ^{241}Am irradiation source, measured at the cell surface, was 3.5MeV and the particles were delivered at a dose rate of $1.0cGy\cdot s^{-1}$. The dose response survival curve of AG1522 showed D_{37}=0.317Gy and D_{50}=0.221Gy when analyzed using the linear-quadratic model (26). During irradiation, 75% of the rectangular dish was shielded with 100μm-thickness aluminum below the dish and cells on another 25% area were irradiated with the doses of 0, 0.5, 1 and 10cGy, respectively (Figure 1). Control dishes went through the same irradiation procedure but 100% shielded. After irradiation, all dishes were removed to the incubator for 30 min and fixed for immunochemical staining.

To investigate the kinetics of the bystander effects induced in the cells of irradiated and unirradiated areas, and for analysis of the time-dependent relationships, cells on 25% of the rectangular dish were irradiated with the dose of 1cGy and then moved to the incubator for the designed time points of 2-360min before fixing and staining to assess the levels of DSBs positive cells.

Treatment with Lindane or Dimethyl Sulfoxide

It has been shown that there are two pathways involved in radiation-induced bystander responses, that is, the pathways involved some medium derived soluble factors such as short-lived reactive oxygen species (ROS) and those that are mediated by GJIC. To examine the mechanisms underlying the bystander effects accessed by the induction of DSBs in unirradiated bystander areas, all cells in

the dish were treated either with 40μM lindane (Sigma) 2h before, during and 30min after irradiation or with 1% (v/v) dimethyl dioxide (DMSO) 15min before, during and 30min after 25% of the area was irradiated with 1cGy α-particles. After treatment, cells were fixed 30min post irradiation to visualize the levels of DSBs. The dose of the two chemicals used is effective and has previously been shown to be non-toxic and non-genotoxic to the cells under the condition used in present studies (8, 27, 28).

*Immuno*chemical *Staining of Cells (γ-H2AX) and DSBs Measurement*

Immunochemical staining of cells was performed as described (29). Briefly, at designated time after irradiation, culture were removed from the incubator, washed with PBS three times, fixed in a 2% paraformaldehyde solution in PBS for 15min at room temperature and then rinsed three times with PBS again. Prior to immunochemical staining, cells were incubated for 30min in TNBS solution (PBS supplemented with 0.1% Triton-X 100 and 1% FBS) to improve their permeability and then incubated with anti-γ-H2AX antibody (Upstate biotechnology, USA) in PBS^+ (PBS supplemented with 1% FBS) for 90min, washed in TNBS for 3×5min, and incubated in PBS^+ for 60min containing the FITC-conjugated goat anti-mouse secondary antibody (Sigma). After another wash with TNBS for 3×5min, cells were counter stained with Hoechst33342 (5μg/ml for 20 min at room temperature). After washing again with TNBS, the stained cells were mounted by 50% of glycerol-carbonate buffer (pH 9.5) for microscopy.

The rectangular Mylar dishes containing the stained cells were placed into one 35-mm-diameter glass bottom dish (glass thickness: 0.17mm, Netherlands) where the outline of rectangular mylar was traced of the glass dish and divided equally into four small sections ($2.5\times6mm^2$) corresponding to the rectangular mylar dish (Figure 1). Immunofluorescence images of cells in irradiated and unirradiated areas (noted as By I (0-2.5mm), By II (2.5-5mm), By III (5-7.5mm to the irradiated area)) were captured with a confocal laser scanning microscope (Lecia, TCS SP2). The captured images on By I area was at least 0.5mm away from the irradiated area to avoid any secondary, scattered particles. Each area was recorded in 4 images and at least 150 cells in each image were counted. For quantitative analysis, the cells with γ-H2AX foci were regarded as the positive cells and the fraction of positive cells was calculated (cells with DSBs / total cells) (30, 31).

Statistical Analysis of Data

Data were presented as mean and standard deviations of the mean from at least three independent experiments with at least twice replicate dishes per experiment. Significant levels were assessed using Student's t-test. A p value of 0.05 or less between groups was considered to be significant.

RESULTS

Induction of DSBs in Irradiated and bystander cells

Approximately 25% of the confluent AG1522 cell monolayers located in one end of the rectangular dishes were irradiated with 0, 0.5, 1 and 10cGy of α-particles and fixed 30min after incubation. The γ-H2AX foci, a biomarker for DSBs in the cells, induced by α-particles or generated endogenously are shown in Figure 2 (white foci in the grey nucleus region of the three-dimension image). The figures showed that tracks representing α-particles traversal and the site of DSBs in unirradiated bystander area after 10cGy irradiation and in sham-irradiated dish. Our previous studies, together with others, demonstrated that the DSBs formation reached a maximum at 30min after irradiation with α-particles (19, 20, 25). Consequently, in the present studies, we chose 30min as the postirradiation incubation time to analyses the dose effect on DSBs formation in the bystander cells.

Figure 3 shows the fraction of DSBs positive cells induced with 0, 0.5, 1 and 10cGy of α-particles on both the irradiated and unirradiated bystander areas. The fraction of DSBs positive cells induced in the irradiated area showed a dose dependent increase in yield. In cells that were irradiated with dose of 0.5 or 1cGy, the fraction of DSBs positive cells was 0.363 and 0.422, respectively, in irradiated area. These yields were significantly greater than those observed in the sham-irradiated cells ($p < 0.01$ for both 0.5cGy and 1cGy dose), and also higher than the proportion of whose nuclei were estimated to be hit. Based on a measured nuclear and cytoplasmic areas of 163±5 μm^2 and 1371±4 μm^2 for the fibroblasts, the percentage of cell nuclei and whole intact cells estimated to be traversed by an α-particles was 4.6% or 38.8% for 0.5cGy and 9.2% or 77.7% for 1cGy (25). Our previous study has suggested that the cytoplasmic or extranuclear contribution to the increase in DSB foci was minimal (25).

The level of DSBs positive cells in unirradiated bystander areas By I, By II and By III all increased 30min after irradiation. However, the increases were not in a dose-dependent manner, and the average percentages of cells containing γ-H2AX foci in the three unirradiated bystander areas are 0.251, 0.251 and 0.259 for the doses of 0.5, 1 and 10cGy, respectively. There was no statistically significant difference in the incidence of γ-H2AX positive cells among unirradiated bystander areas. Compared to the sham-irradiation control cells, the increases in DSBs in both the irradiated and in the unirradiated areas were all significantly different ($p<0.01$). These results are consistent with published studies using different endpoints (14-16) and suggested that the

bystander effects could be induced in unirradiated cells when co-cultured with the irradiated ones.

The Time and Spatial Effects of DSBs Induction in Bystander Cells

To detect the time effect of DSBs induction, 25% of the confluent AG1522 cell monolayers located in one end of the rectangular dishes were irradiated with 1cGy dose of α-particles and the cultures were fixed at designated time for the immunohistochemical staining of γ-H2AX foci. Figure 4 shows that the fraction of induced DSB positive cells in irradiated area varied with the post-irradiation incubation time and was significantly higher than sham-irradiated controls at all time points examined ($p<0.01$). By 2 min after irradiation, the fraction of DSBs in By I of the unirradiated bystander area, which is closest to the irradiated section, was already significantly higher than the corresponding sham-irradiated control ($p< 0.01$). In contrast, in By II and By III, no such differences in the fraction DSBs were detected yet (figure 4). By 6 min post-irradiation, the percentage of DSBs in both By I and By II showed a progressive increase over the controls whereas no increase was observed among the bystander cells in By III until 10 min post-irradiation when compared with the corresponding sham-irradiated controls in that zone. From 15 min to the 360 min observational period when the fractions of DSBs in each zone were monitored, the bystander DSBs in the various unirradiated areas were all significantly higher than the corresponding controls ($p<001$ or $p<0.05$ as indicated). Furthermore, by 30 minutes post-irradiation, the incidence of DSBs reached a maximum for both the directly irradiated and bystander cells. With further increase in time, the fractions of DSBs in both irradiated and unirradiated bystander areas gradually decreased. However, by 360 min post-irradiation, the incidence of DSBs in both of these areas, including the three bystander zones, remained significantly higher than their respective controls.

Attenuation of DSBs Formation by Lindane or DMSO treatment

Pretreatment of cells with either the gap junction communication inhibitor lindane (40 μM) or with the free radical scavenger dimethyl dioxide (1%) reduced the fraction of DSB positive cells both in the irradiated and unirradiated bystander areas (Figure 5). In cells irradiated with 1cGy dose of α-particles, addition of lindane and DMSO reduced the number of cells containing γ-H2AX foci by 48.1% and 56.2% in irradiated area, from 42.2% to 21.9% and 18.5%, respectively ($p<0.01$). Similar results were also obtained among cells in three unirradiated bystander areas as well, and the average decreases were about 32.5% (lindane) and 38.5%

(DMSO) from 26.2% to 17.7% and 16.1%, respectively (p<0.01). The decrease in DSB positive cells after treatment with chemical agents suggested that GJIC or ROS might play important roles in the induction of bystander effect both in irradiated and unirradiated bystander areas.

DISCUSSION

Radiation-induced bystander effects have been extensively studied in the past decade (1, 3, 4). The plethora of data now available concerning this effect fall into two categories: 1) in confluent cultures where physical contacts between irradiated and non-irradiated cells are made and where gap junctional communications have been shown to be essential for the process; and 2) in sparsely populated cultures where bystander effects may be mediated by damage signals released into the culture medium by the irradiated cells. As a result, incubation of non-irradiated cells with conditioned medium from irradiated cultures may lead to induction of biological effects. In the present study, confluent monolayers of AG1522 normal human diploid fibroblasts were used. It is not clear if the signaling molecules involved in the two bystander processes are mutually exclusive. In fact, it is likely that some common initiating or intermediate steps are involved. *In situ* DSBs assay, based on the immunohistochemical staining of γ-H2AX, can reflect the DSBs induction as early as 1min after irradiation (19, 20). Compared with other endpoints in bystander studies, it provides a fast and real-time method to analyze the transfer of bystander signal, as well as kinetics of the RIBE.

Our results of fixing and staining the cells 30min after irradiation show that the bystander signals initiated by very low doses of α-particles in irradiated cells can induce the DSBs damage in the unirradiated bystander cells far away from the irraidated areas (7.5mm, the longest distance in our experiment system). That is to say, the RIBE can influence any cells in the co-culture dish. This result is consistent with the findings of Belyakov *et al*. (14) and Schettino *et al*. (15), showing that a cell has the same chance of responding to the bystander signals whatever its distance. Moreover, using the *in situ* DSBs assay, the average levels of DSBs damage in unirradiated bystander areas, after irradiation with the graded doses of α-particles, were about 2-fold higher than that of the controls. No dose-dependent effect was found in unirradiated bystander cells. Such saturation effect was similar to the findings of Ponnaiya *et al*. (32-34), showing that the lack of a dose dependent response in the induction of MN and chromosomal aberration in unirradiated cells and its progeny.

Our results further demonstrated that the formation of DSBs occurred very soon after irradiation and the yields of DSBs positive cells in both irradiated and unirradiated bystander areas showed a time dependent increase during the 0-30min postirradiation period. Although there is the tendency that DSBs induction decreases after 30min post irradiation, the inductions of

DSBs at 60, 180 and 360min after irradiation are still significantly high than their corresponding controls, and maintains steady (Figure 4). The decrease of DSBs induction both in irradiated and unirradiated areas 30min post irradiation might be due to the repair process initiated in cells (35, 36). There is evidence that after exposure of IMR90 cells to 12Gy γ-rays, γ-H2AX foci appeared in 100% of the cell population rapidly, in contrast, Rad50 foci appeared more slowly, over a period of several hours (6–8 hours post-irradiation) (37). Replication protein A (RPA) plays important roles in DNA replication, repair, and recombination. Coincidence of RPA and γ-H2AX foci was detectable at 30 min after IR, but the exact coincidence detected at 2 h after γ-rays indicated a time-dependent association of both proteins at the DSB sites (38). Those un-repaired DSBs might further involve in the induction of SCE, MN, mutation and cancer incidence in the future (39, 40). The study of Rothkamm *et al* also demonstrated that the un-repaired DSBs which was ＜1 DSB per cell, induced by low dose γ-irradiation, could persisted for days (41).

It is of interest to observe that at very early stage (2-6 min) post-irradiation, the induction of DSBs shows a distance dependent increase, that is, the zone closest to the irradiated area shows the earliest induction of bystander effect (Figure 4). However, 10min after irradiation, the fraction of DSBs induced in unirradited bystander areas was all significantly different from their corresponding controls and showed the damaged cells in bystander areas distributing uniformly over the areas of the dish scanned. These results might suggest that the transmission of RIBE is a distance dependent phenomenon as the bystander signal is propagated across the various zones. To the best of our knowledge, this is the first time report that demonstrates the kinetics in the transmission of RIBE.

The mechanism of RIBE, whether involving cell-cell contact or mediated by soluble factors, is not clear and is likely to be complex and involves multiple pathways. In sub-confluent cultures, there is evidence that reactive oxygen species, cytokines such as TGF_{β}, and nitric oxide are essential in mediating the process (1). On the other hand, gap junction mediated cell-cell communications have been shown to be critical in mediating the bystander effects in confluent cultures of either human (27, 42) or rodent cells (8, 9). In the present study, the results of using of lindane, inhibitor of GJIC, or DMSO, scavenger of ROS, which all decreased the fraction of DSB positive cells (Figure 5) both in irradiated and unirradiated bystander areas, suggests that GJIC or ROS might both play important roles in the induction of bystander effect. It is likely that multiple signaling cascades involving both an initiating event and downstream signaling steps are

necessary to mediate the bystander process, and a combination of pathways involving both primary and secondary signaling processes is involved in the bystander process. There is evidence that certain cytokines such as TGF_{β} may be involved in the bystander signaling process (43). Recent findings by one of the coauthors have demonstrated that cyclooxygenase-2 (COX-2) signaling cascade plays an essential role in the bystander process. Treatment of bystander cells with NS-398, which suppresses COX-2 activity, significantly reduced the bystander effect (44). It is likely that both radical species and gap junctional mediated process contribute to the bystander effects as our results indicated.

ACKNOWLEDGMENTS

The authors are grateful to Dr. Haiying Hang for his technical assistance with DSBs detection. This work was funded by National Nature Science Foundation of China under Grant No. 10225526 and 30070192, and Grant KSCX2-SW-324 of Chinese Academy of Sciences.

REFERENCES

1. Hei, T. K., Persaud, R., Zhou, H., and Suzuki, M. (2004) Genotoxicity in eyes of bystander cells. *Mutation Research,* **568**, 111-120 (review).

2. Nagasawa, H., and Little, J. B. (1992) Induction of sister chromatid exchanges by extremely low doses of alpha-particles. *Cancer Res.*, **52,** 6394–6396.

3. Hall, E. J., and Hei, T. K. (2003) Genomic instability and bystander effects induced by high-LET radiation. *Oncogene*. **22(45)**, 7034-7042 (review).

4. Mothersill, C., and Seymour, C.B. (2004) Radiation-induced bystander effects-implications for cancer, *Nat. Rev. Cancer*, **4**, 158–164 (review).

5. Sawant, S. G., Randers-Pehrson, G., Geard, C. R., Brenner, D. J., and Hall, E. J. (2001) The bystander effect in radiation oncogenesis: I. Transformation in C3H 10T1/2 cells in vitro can be initiated in the unirradiated neighbors of irradiated cells. *Radiat. Res.*, **155,** 397-401.

6. Prise, K. M., Belyakov, O. V., Folkard, M., and Michael, B. D. (1998) Studies on bystander effects in human fibroblasts using a charged particle microbeam. *Int. J. Radiat. Biol.*, **74,** 793-798.

7. Azzam, E. I., De Toledo, S. M., Spitz, D. R., and Little, J. B. (2002) Oxidative metabolism modulates signal transduction and micronucleus formation in bystander cells from alpha-particles-irradiated normal human fibroblast culture. *Cancer Res.*, **62,** 5436-5442.

8. Zhou, H., Randers-Pehrson, G., Waldren, C. A, Vannais, D., Hall, E. J, and Hei, T. K. (2000) Induction of a bystander mutagenic effect of alpha particles in mammalian cells. *Proc Natl Acad Sci U S A*, **97(5)**, 2099-2104.

9. Zhou, H., Suzuki, M., Randers-Pehrson, G., Vannais, D., Chen, G., Trosko, J. E., Waldren, C. A, and Hei, T. K. (2001) Radiation risk to low fluences of alpha particles may be greater than we thought. *Proc. Natl. Acad. Sci. USA,* **98,** 14410–14415.

10. Mothersill, C., and Seymour, C. (1997) Medium from irradiated human epithelial cells but not human fibroblasts reduces the clonogenic survival of unirradiated cells. *Int. J.*

Radiat. Biol., **71,** 421-427.

11. Maguire, P., Mothersill, C., Seymour, C., and Lyng, F. M. (2005) Medium from irradiated cells induces dose-dependent mitochondrial changes and BCL2 responses in unirradiated human keratinocytes. *Radiat Res*, **163(4)**, 384-390

12. Mothersill, C., and Seymour, C. (2002) Bystander and delayed effects after fractionated radiation exposure. *Radiat Res.,* **158(5),** 626-633.

13. Bishayee, A., Hill, H. Z., Stein, D., Rao, D. V., and Howell, R. W. (2001) Free radical-initiated and gap junction-mediated bystander effect due to nonuniform distribution of incorporated radioactivity in a three-dimensional tissue culture model. *Radiat. Res.*, **155**, 335-344

14. Belyakov, O. V., Malcolmson, A. M., Folkard, M., Prise, K. M., and Michael, B. D. (2001) Direct evidence for a bystander effect of ionizing radiation in primary human fibroblasts. *Br. J. Cancer*, **84,** 674–679.

15. Schettino, G., Folkard, M., Prise, K. M., Vojnovic, B., Held, K. D., and Michael, B. D. (2003) Low-dose studies of bystander cell killing with targeted soft X-rays. *Radiat. Res.,* **160,** 505-511.

16. Hill, M. A., Ford, J. R., Clapham, P., Marsden, S. J., Stevens, D. L., Townsend, K. M. S., and Goodhead, D. T. (2005) Bound PCNA in nuclei of primary Rat Tracheal Epithelial Cells after Exposure to Very Low Doses of Plutonium-238 α Particles. *Radiat. Res.*, **163,** 36-44.

17. Hoeijmakers, J. H. (2001) Genome maintenance mechanisms for preventing cancer. *Nature*, **411,** 366–374.

18. Hall, Eric J. (1994) *Radiobiology for the Radiologist*. 4th edition. J. B. Lippincott Company, pp.16-17.

19. Rogakou, E. P., Pilch, D. R., Orr, A. H., Ivanova, V. S., and Bonner, W. M. (1998) DNA double-stranded breaks induce histone H2AX phosphorylation on serine 139. *J. Biol. Chem.*, **273,** 5858-5868.

20. Rogakou, E. P., and Pilch, D. R. (1999) Megabase chromatin domains involved in

DNA double-strand breaks in vivo. *J. Cell Biol.*, **146,** 905-915.

21. Burma, S., Chen, B. P., Murphy, M., Kurimasa, A., and Chen, D. J. (2001) ATM phosphorylates histone H2AX in response to DNA double-strand breaks. *J. Bio. Chem.*, **276,** 42462-42467.

22. Chen, H. T., Bhandoola, A., Difilippantonio, M. J., Zhu, J., Brown, M. J., Tai, X., Rogakou, E. P., Brotz, T. M., Bonner, W. M., Ried, T., and Nussenzweig, A. (2000) Response to RAG-mediated VDJ cleavage by NBS1 and gamma-H2AX. *Science*, **290,** 1962-1965.

23. Petersen, S., Casellas, R., Reina-San-Martin, B., Chen, H. T., Difilippantonio, M. J., Wilson, P. C., Hanitsch, L., Celeste, A., Muramatsu, M., and Nussenzweig, A. (2001) AID is required to initiate Nbs1/gamma-H2AX focus formation and mutations at sites of class switching. *Nature*, **414,** 660-665.

24. Mahadevaiah, S. K., Turner, J. M., Baudat, F., Rogakou, E. P., de Boer, P., Blanco-Rodriguez, J., Jasin, M., Keeney, S., Bonner, W. M., and Burgoyne, P. S. (2001) Recombinational DNA double-strand breaks in mice precede synapsis. *Nat. Genet.*, **27,** 271-276.

25. Hu, B., Han, W., Wu, L., Feng, H., Liu, X., Zhang, L., Xu A., Hei, T. K and Yu, Z. (2005) *In situ* visualization of DSBs to assess the extranuclear/extracellular effects induced by low dose α-particle irradiation. *Radiat. Res.*, **164 (3)**, 286-293.

26. Hu, B., Wu, J., Han, W., Wang, X., Wu L., and Yu, Z. (2005) Development of a dose-adjustable α-particle irradiation facility for radiobiological studies. *Nuclear Science and Techniques.* 16(2), 102-107.

27. Azzam, E. I., de Toledo, S. M., and Little, J. B. (2001) Direct evidence for the participation of gap junction-mediated intercellular communication in the transmission of damage signals from α-particle irradiated to nonirradiated cells. *Proc. Natl. Acad. Sci. U S A*, **98,** 473-478.

28. Narayanan, P. K., Goodwin, E. H., and Lehnert, B. E. (1997) Alpha particles initiate biological production of superoxide anions and hydrogen peroxide in human cells. *Cancer Res.*, **57,** 3963-3971.

29. Aten, J. A., Stap, J., Krawczyk, P. M., van Oven, C. H., Hoebe, R. A., Essers, J., and Kanaar, R. (2004) Dynamics of DNA double-strand breaks revealed by clustering of damaged chromosome domains. *Science*, **303(5654)**, 92-95.

30. Limoli, C. L., Giedzinski, E., Bonner, W. M., and Cleaver, J. E. (2002) UV-induced replication arrest in the xeroderma pigmentosum variant leads to DNA double-strand breaks, gamma -H2AX formation, and Mre11 relocalization. *Proc Natl Acad Sci U S A*, **99(1),** 233-238.

31. d'Adda di Fagagna, F., Reaper, P. M., Clay-Farrace, L., Fiegler, H., Carr, P., Von Zglinicki, T., Saretzki, G., Carter, N. P., and Jackson, S. P. (2003) A DNA damage checkpoint response in telomere-initiated senescence. *Nature*, **426(6963)**, 194-198.

32. Ponnaiya, B., Cornforth, M. N., and Ullrich, R. L. (1997) Induction of chromosomal instability in human mammary cells by neutrons and γ-rays. *Radiat. Res.*, **147,** 288-294

33. Ponnaiya, B., Jenkins-Baker, G., Brenner, D. J., Hall, E. J, Randers-Pehrson, G., and Geard, C. R. (2004) Biological responses in known bystander cells relative to known microbeam-irradiated cells. *Radiat Res*., **162(4)**, 426-432.

34. Ponnaiya, B., Jenkins-Baker, G., Bigelow, A., Marino, S., and Geard, C., R. (2004) Detection of chromosomal instability in α-irradiated and bystander human fibroblasts. *Mutation Research*, **568**, 41-48.

35. Rothkamm, K., Krüger, I., Thompson, L, H., Löbrich, M. (2003) Pathways of DNA double-strand break repair during the mammalian cell cycle. *Molecular and cellular biology*, **23(16)**, 5700-5715.

36. Nazarov, I. B., Smirnova, A. N., Krutilina, R. I., Svetlova, M. P., Solovjeva, L. V., Nikiforov, A. A., Oei, S-L, Zalenskaya, I. A., Yau, P. M., Bradbury, E. M., and Tomilin, N. V. (2003) Dephosphorylation of histone γ-H2AX during repair of DNA double-strand breaks in mammalian cells and its inhibition by calyculin A. *Radiat. Res.,* **160**, 309-317

37. Paull, T. T., Rogakou, E. P., Yamazaki, V., Kirchgessner, C. U., Gellert, M., and Bonner, W. M. (2000) A critical role for histone H2AX in recruitment of repair factors to nuclear foci after DNA damage. *Curr Biol.,* **10(15)**, 886-895.

38. Balajee, A. S., and Geard, C. R. (2004) Replication protein A and gamma-H2AX

foci assembly is triggered by cellular response to DNA double-strand breaks. *Exp Cell Res.,* **300(2)**, 320-334.

39. Petukhova, G., Stratton, S., and Sung, P. (1998) Catalysis of homologous DNA pairing by yeast Rad51 and Rad54 proteins. *Nature*, **393**, 91–94

40. Fenech, M. (2000) The in vitro micronucleus technique. *Mutat. Res.,* **455**, 81-95

41. Rothkamm, K., and Lobrich, M. (2003) Evidence for a lack of DNA double-strand break repair in human cells exposed to very low x-ray doses. *Proc Natl Acad Sci U S A.*, **100(9)**, 5057-5062

42. Shao, C., Furusawa, Y., Kobayashi, Y., Funayama, T., and Wada, S. (2003) Bystander effect induced by counted high-LET particles in confluent human fibroblasts: a mechanistic study. *FASEB J.*, **17(11)**, 1422-1427.

43. Iyer, R., Lehnert, B. E., and Svensson, R. (2000) Factors underlying the cell growth-related bystander responses to alpha particles. *Cancer Res.,* **60(5)**, 1290-1298

44. Zhou, H., Ivanov, V. N., Gillespie, J., Geard, C. R., Amundson, S. A., Brenner, D. J., Yu, Z., Lieberman, H. B., and Hei T. K. (2005) Mechanism of Radiation-Induced Bystander Effect: Role of COX-2 Signaling Pathway. *Proc Natl Acad Sci U S A.* in press.

Legends to Figures

FIG. 1. Schematic diagram of the Mylar dish used in the study for irradiation and image capturing. The specially designed dish (internal area: 10×6 mm^2) consists of a 3.5 μm thick Mylar film bottom on which cells attached. The unirradiated cells were shielded with aluminum (left hand panel). The images were captured in the irradiated area and the unirradiated areas when the Mylar dishes containing the stained cells were placed on the 35-mm-diameter glass bottom dish where the partial of the mylar dish was marked and divided equally into four small sections (2.5×6mm^2) as By I, By II and By III corresponding to the rectangular mylar dish (right hand panel).

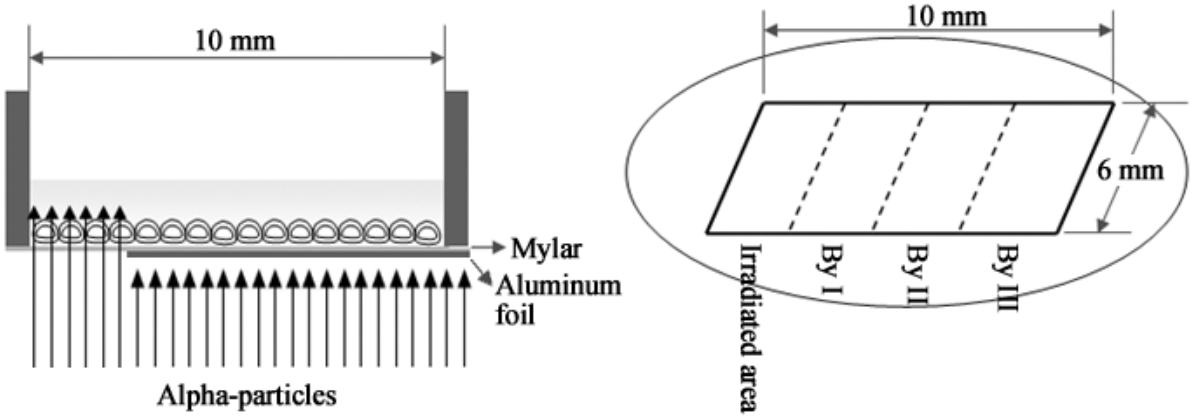

FIG.2. Induction of DSBs in irradiated and unirradiated bystander cells. Representative image of DSB positive cells (white γ-H2AX foci in the grey nucleus region) in sham irradiated dish (A), 10cGy α-particle irradiated area (B) and bystander area (C).

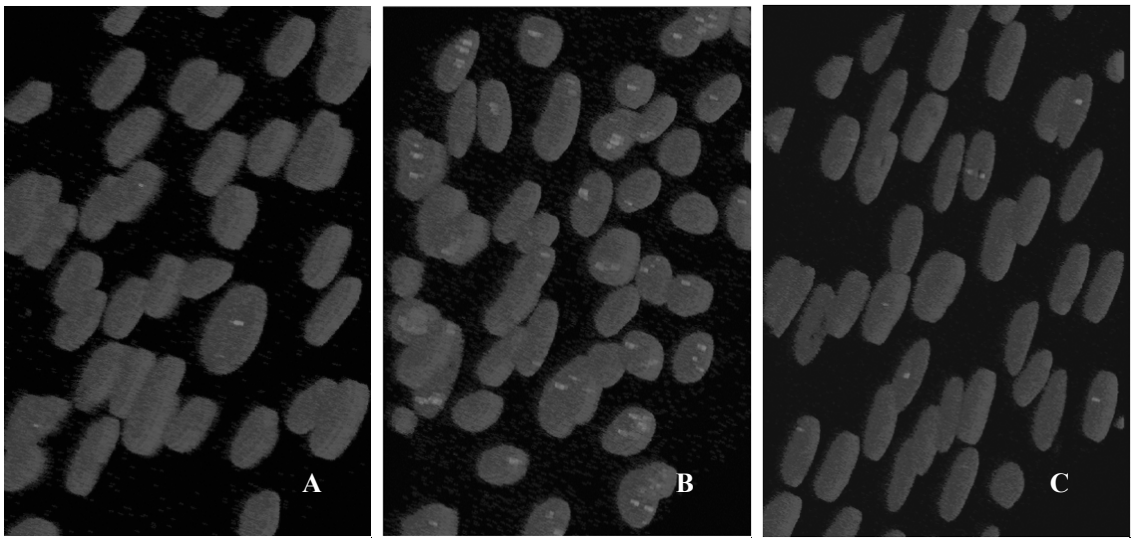

FIG.3. Induction of DSBs in irradiated and unirradiated bystander fibroblasts. The fractions of DSBs positive cells were calculated 30min after irradiation with 0, 0.5, 1 and 10cGy of α-particles. Data were pooled from 5 individual experiments. Error bars represent the standard deviations of the means. The symbol * depicts values are statistical significant (p<0.01) between the corresponding controls and the experiment groups.

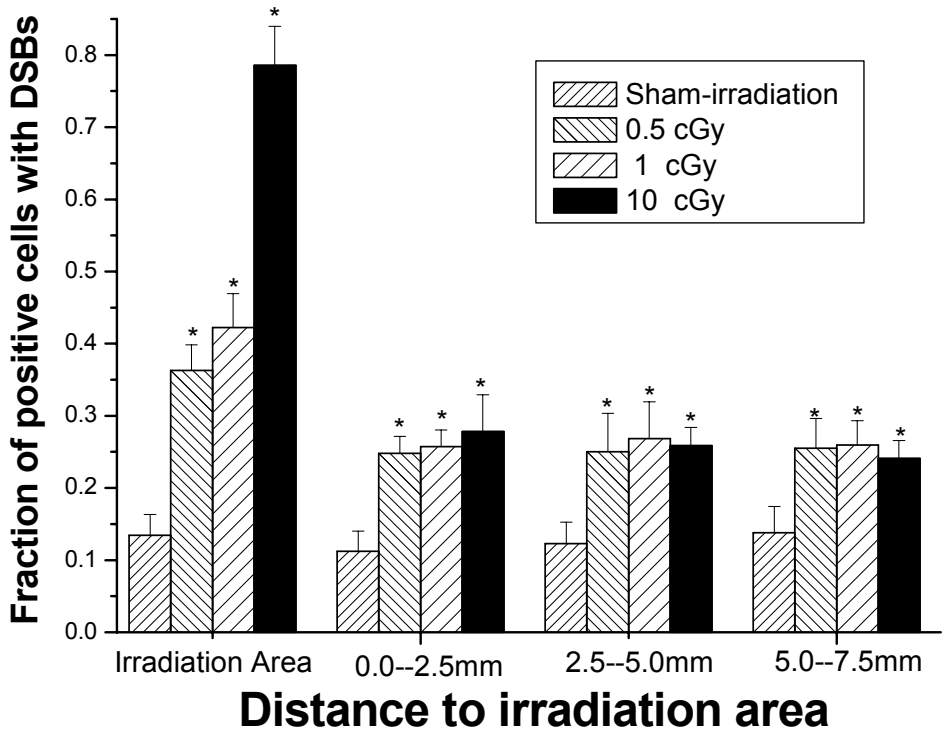

FIG. 4. Bystander DSBs induction response as a function of time and distance from irradiated cells in primary human fibroblasts. The fractions of DSBs positive cells were calculated 2, 6, 10, 15, 30, 45, 60, 180 and 360min after irradiation with 1 cGy of α-particles. Data were pooled from 3 individual experiments. Error bars represent the standard deviations of the means. The symbol * and ** depicts values are statistical significant (p<0.05 and p<0.01, respectively) between the corresponding controls and the experimental groups.

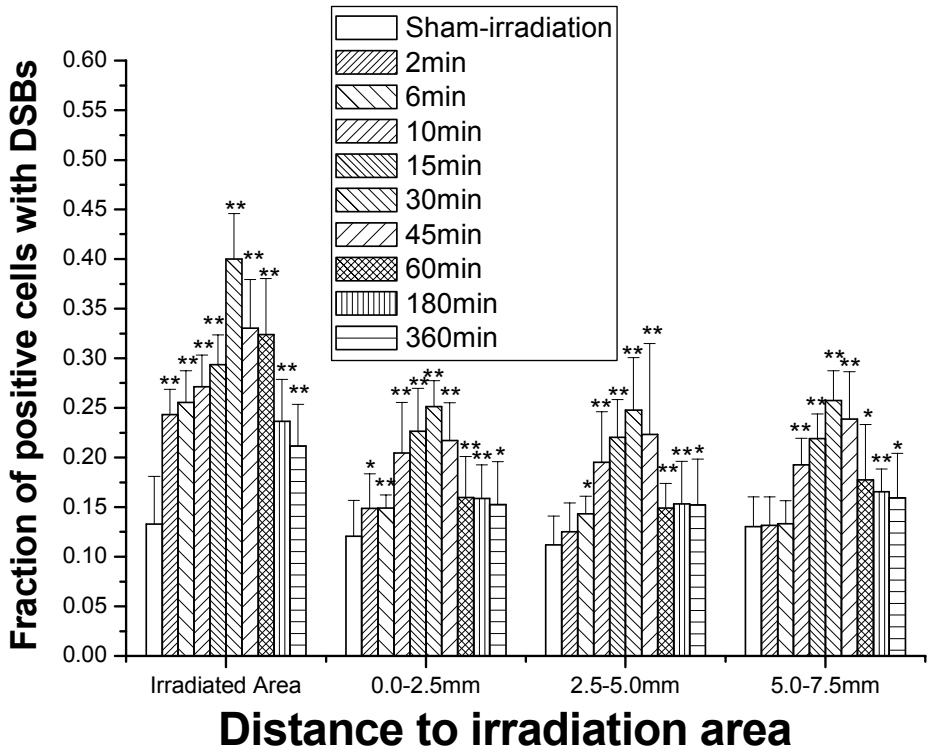

FIG.5. The fraction of DSBs positive cells induced by 1cGy of α-particle irradiation treated with or without 40μM lindane (a) or 1% DMSO (b). Data were pooled from 4 individual experiments. Error bars represent the standard deviations of the means. The symbol * depicts values that are statistical significant (p<0.01) between the lindane and DMSO treated and without treated groups.